(treated as HF MO's), two Ru–C bond pairs each with a second NO for a total of four Ru–C bonding orbitals, one doubly occupied nonbonding $d\bar{\pi}_{yz}$ orbital, and three singly occupied $d\sigma$, $d\delta$, $d\bar{\delta}$ orbitals, for a total of 10 orbitals in the valence space. At the GVB(2/4)-PP level for $RuCH_2^+$ ($^2A_2$), there is the same orbital space for CH_2 and for the Ru–C bonds, but there are two doubly occupied nonbonding d orbitals ($d\pi_{yz}$ and $d\delta_{x^2-y^2}$) plus one singly occupied $d\delta_{xy}$ orbital, for a total of nine valence orbitals. To treat the states of $RuCH_2^+$ with the same degree of flexibility, we must have the same number of valence orbitals in the SCF calculations. Therefore, for $RuCH_2^+$ ($^2A_2$) we correlate the $d\delta_{x^2-y^2}$ with a second natural orbital (leading to a GVB(3/6)-PP description) in order to compare with the GVB(2/4)-PP description of $RuCH_2^+$ ($^4A_2$).

Acknowledgment. This work was supported by the Shell Development Company, Houston, TX, and the National Science Foundation (Grant No. DMR82-15650).

Registry No. $Ru{=}CH_2^+$, 101031-94-1.

Thermal Decomposition of Silane

Mark S. Gordon,*† David R. Gano,‡ J. Stephen Binkley,⊥ and Michael J. Frisch‖

Contribution from the Department of Chemistry, North Dakota State University, Fargo, North Dakota 58105, Department of Chemistry, Minot State College, Minot, North Dakota, Sandia National Laboratory, Livermore, California 94550, and Analytical Sciences Division, Kodak Research Laboratories, Rochester, New York 14650.
Received September 13, 1985

Abstract: The essential features of the potential energy surface for the thermal decomposition of silane have been calculated with extended basis sets, augmented by correlation corrections. It is predicted that the transition state for the molecular elimination lies 56.9 kcal/mol above silane. For the reverse reaction, the transition state is less than 2 kcal/mol above the separated fragments, silylene and molecular hydrogen, but 4.8 kcal/mol above a long-range potential well. In the latter, the silylene–H_2 separation is 1.78 Å, and the bond in H_2 has stretched by more than 0.05 Å. This indicates a significant electronic interaction between the fragments even at the large fragment separation. The depth of the well is less than 1 kcal/mol at the SCF level of theory, but it increases substantially when correlation is introduced into the wave function. Since the calculated SiH bond energy is 22 kcal/mol larger than the activation energy for the molecular elimination, the homolytic cleavage of silane to form silyl radical is not expected to be an important process in the low-energy pyrolysis of silane.

I. Introduction

The mechanism of the thermal decomposition of silane is of considerable current interest. Silane decomposition is the initial chemical step in the chemical vapor deposition (CVD) of silicon on surfaces. At low temperatures, the primary decomposition process in silane pyrolysis is the elimination of molecular hydrogen to form silylene.[1]

$$SiH_4 \rightarrow SiH_2 + H_2 \qquad (1)$$

The latter species is the simplest example of divalent silicon, a class of compounds with great mechanistic importance in organosilicon chemistry. In the current context, for example, silylene may insert into an Si–H bond of the parent to form disilane, thereby allowing the study of the thermal decomposition mechanisms of this molecule as well.[2]

John and Purnell[3] (JP) have estimated the heat of formation of silylene to be 57.9 kcal/mol, while O'Neal and Ring[4] (OR), based on their silane and disilane pyrolysis experiments, find just over 58 kcal/mol for this quantity. Combined with the heat of formation of 8.2 kcal/mol for silane,[5] this suggests that the endothermicity of (1) is about 50 kcal/mol. JP and OR estimate the activation energy E_a for the insertion of silylene into H_2 [the reverse of (1)] to be 5 and 8 kcal/mol, respectively. This suggests a decomposition barrier of 55–58 kcal/mol for silane. Jasinski and Estes,[6a] using the technique of laser powered homogeneous pyrolysis, have directly determined the latter E_a to be 52 ± 7 kcal/mol and have very recently determined the activation energy for the insertion of silylene into D_2 to be 1 kcal/mol.[6b]

There have been several theoretical studies of reaction 1. Viswanathan, Thompson, and Raff[7] (VTR) have used a semi-empirical potential energy surface to predict the kinetics of the unimolecular decomposition of silane and concluded that the channel corresponding to homolytic cleavage of one SiH bond only becomes important at internal silane energies in excess of 5.0 eV. Gordon,[8] using second-order Møller–Plesset perturbation (MP2) theory and the 6-31G* basis set,[9] found an insertion barrier of 8.6 kcal/mol. With third-order perturbation theory (MP3) and polarization functions on the hydrogens (6-31G** basis set[9]), the barrier is reduced to 5.5 kcal/mol.[10] Correcting for zero-point vibrational contributions raises these values by about 2 kcal/mol, resulting in activation energies of 10.6 and 7.5 kcal/mol, respectively. The latter value is within the range of the experimental estimates.

Using a double-ζ plus polarization basis set, Grev and Schaefer[11] (GS) have studied reaction 1 with a two-configuration multiconfigurational self-consistent-field (MCSCF) wave function, augmented by second-order configuration interaction (SOCI). This 7000 configuration wave function predicts a 6.8 kcal/mol

† North Dakota State University.
‡ Minot State College.
⊥ Sandia National Laboratory.
‖ Kodak Research Laboratories.

(1) (a) Purnell, J. H.; Walsh, R. *Proc. R. Soc. London* **1966**, *A293* 543. (b) Neudorfl, P.; Jodhan, A.; Strausz, O. P. *J. Phys. Chem.* **1980**, *84*, 338. (c) Newman, C. G.; O'Neal, H. E.; Ring, M. A.; *Leska*, E. F.; Shipley, N. *Int. J. Chem. Kinet.* **1979**, *11*, 1167.
(2) Olbrich, G.; Potzinger, P.; Reimann, B.; Walsh, R. *Organometallics* **1984**, *3*, 1267.
(3) John, P.; Purnell, J. H. *J. Chem. Soc., Faraday Trans. 1*, **1973**, *69*, 1455.
(4) O'Neal, H. E.; Ring, M. A. *Chem. Phys. Lett.* **1984**, *107*, 442.
(5) Chase, M. W.; Curnutt, J. L.; Downey, J. R.; McDonald, R. A.; Syverud, A. N.; Valenzuela, E. A. *J. Phys. Chem. Ref. Data* **1982**, *11*, 695.
(6) (a) Jasinski, J. M.; Estes, R. D. IBM Research Report No. 49067, 1985. (b) Jasinski, J. M. *J. Phys. Chem.*, submitted.
(7) Viswanathan, R.; Thompson, D. L.; Raff, L. M. *J. Chem. Phys.* **1984**, *80*, 4230.
(8) Gordon, M. S. *J. Chem. Soc., Chem. Commun.* **1981**, 890.
(9) Hariharan, P. C.; Pople, J. A. *Theor. Chim. Acta* **1973**, *28*, 213. Gordon, M. S. *Chem. Phys. Lett.* **1980**, *76*, 163.
(10) Gordon, M. S.; Gano, D. R. *J. Am. Chem. Soc.* **1984**, *106*, 5421.
(11) Grev, R. S.; Schaefer, H. F., III *J. Chem. Soc., Chem. Commun.* **1983**, *14*, 785.

0002-7863/86/1508-2191$01.50/0

activation energy, again in good agreement with the experimental data. Because there are four active orbitals in the insertion process and four active electrons, Gordon and Gano[10] expanded the MCSCF wave function used by GS to 20 configurations, again augmented by SOCI (denoted SOCI/MCSCF(4,4)/6-31G*). The resulting activation energy of 10.4 kcal/mol is somewhat higher than the GS result, and the difference was attributed to the omission of polarization functions on the hydrogens in the Gordon–Gano paper. Indeed, assuming additivity of the effects of correlation and polarization functions on hydrogen,[12] the SOCI/MCSCF(4,4)/6-31G** activation energy is estimated to be 8.0 kcal/mol.

With regard to the heat of formation, Pople and co-workers[13] and Binkley and Melius[14] have predicted a value of 66–68 kcal/mol, using near Hartree–Fock basis sets and full fourth-order perturbation theory (MP4). The level of these calculations is such that one would expect an error of no more than 2–3 kcal/mol. Indeed, the level of agreement for all other SiH_n and all CH_n is within this range. Thus, there appears to be a serious disagreement between theory and experiment with regard to the heat of formation of SiH_2.

In a related development, Schlegel[15] and the authors[16] have discovered that with split valence plus polarization basis sets augmented by MP2 or MP3 corrections, a long-range well appears on the SiH_4 surface. This apparent minimum is lower in energy than the separated reactants and therefore may have an effect on the observed insertion barrier. Interestingly, the semiempirical calculation by VTR, used to model the dynamics of the silane decomposition, finds at least one pathway for which the insertion barrier is zero and which contains a shallow long-range minimum of about 7 kcal/mol.[7]

Because of the considerable interst in the silane decomposition surface, the present work was initiated to investigate the effect of dramatic improvements in basis set and of improving the level of perturbation theory to fourth order and to further study the apparent long-range minimum on the SiH_4 surface.

II. Methods of Calculation

The transition state for the silylene insertion was initially determined at the SCF/3-21G[17] level of computation, using the GAUSSIAN82 code[18] and the Schlegel scheme for locating transition states.[19] This was subsequently refined with use of the 6-31G* basis set[9] and the 20-configuration fully optimized reaction space (FORS)/MCSCF[20] wave function discussed above. With use of a modified version of GAMESS,[21] the MCSCF(4,4)/6-31G* intrinsic reaction coordinate (IRC)[22] was followed from the transition state toward both reactants and products.

Calculations along the IRC have been carried out at several levels of theory and with several, successively larger basis sets. SOCI/MCSCF(4,4) energies were calculated with use of the 6-31G* basis set, supplemented by p functions on the reacting hydrogens. Third[23] and full fourth[24] order Møller–Plesset perturbation theory calculations (MP3 and MP4) have been performed with the 6-31G** basis,[9] as well as with the following larger basis sets: (A) the unscaled Dunning [2s] double-ζ basis for H[25] plus a set of p functions (scale factor = 1.0), combined with the McLean–Chandler basis set for silicon,[26] including the 6-31G* silicon d exponent;[9] (B) same as A, but with the hydrogen scale factor = 1.2; (C) the McLean–Chandler basis for Si, combined with -311G** for H;[27] and (D) same as C, but with two sets of silicon d functions, chosen from the original single d set according to the Schmidt prescription[28]—the single d set is multiplied by factors of 0.4 and 1.4.

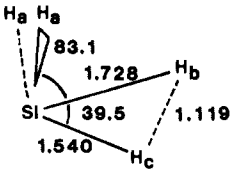

Figure 1. MCSCF structure for the transition state. Bond lengths in Å, angles in degrees. $R(CH_a)$ = 1.483 Å, H_aSiH_c angle = 105.8°.

Finally, the key points (see below) along the IRC have been reoptimized at the MP2 level with the MC-311G (2d,2p) basis set.[29] This has been followed by single point calculations using the MC-311++G (3df,3pd)[29] basis set. In the latter basis set, hereafter referred to as E, the notation (3df,3pd) indicates the addition of three sets of d basis functions and one set of f functions to silicon and the addition of three sets of p basis functions and one set of d functions to the hydrogens. Calculations performed at one computational level (A) using geometries obtained at another (usually lower) computational level (B) are denoted with the notation A//B. Thus the foregoing example would be denoted MP4/MC-311++G(3df,3pd)//MP2/MC-311G(2d,2p).

III. Results and Discussion

The MCSCF(4,4)/6-31G* geometry at the saddle point of reaction 1 is shown in Figure 1. The geometry is rather distorted into C_s symmetry, with the Si–H distances to the two leaving hydrogens being different by nearly 0.2 Å. Such a distorted structure is expected, since the least motion C_{2v} reaction path is "symmetry forbidden".[30]

The SCF, MP2, MP3, and MP4 (SDTQ) energies along the MCSCF/6-31G* IRC are shown in Figure 2, a–d, respectively, for 6-31G** and basis sets A–D (the specific structures used for this calculation are available from the authors upon request). Both the 6-31G** SCF and MCSCF(4,4)/6-31G* curves (not shown) decrease montonically from the transition state to both reactants and products. Improvement of the basis set introduces a small well (see below) in the SCF curve at long separation of the fragments. The introduction of perturbation theory results in a considerable deepening of this long-range potential energy well. The addition of second-order CI to the MCSCF wave function (not shown) introduces a similar well into that curve. It is particularly important to note that the SCF configuration is strongly dominant in the MCSCF wave function at all points along the IRC. Thus, this section of the potential energy surface is well represented by a single configuration-based wave function.

The four key points along the IRC are separated reactants (R), the long-range well (W), the saddle point (S), and the product (P). The calculated total and relative energies at these points are listed in Tables I and II, respectively, for 6-31G** and basis sets A–D as a function of the level of perturbation theory. Since the

(12) (a) Gordon, M. S. *J. Am. Chem. Soc.* **1982**, *104*, 4352. (b) KcKee, M. L.; Lipscomb, W. N. *J. Am. Chem. Soc.* **1981**, *103*, 4623. (c) Holme, T. A.; Gordon, M. S.; Yabushita, S.; Schmidt, M. W. *Organometallics* **1984**, *3*, 583.

(13) Pople, J. A.; Luke, B. T.; Frisch, M. J.; Bunkley, J. S. *J. Phys. Chem.* **1985**, *89*, 2198.

(14) Melius, C.; Binkley, J. S.; unpublished results.

(15) Sosa, C.; Schlegel, H. B. *J. Am. Chem. Soc.* **1984**, *106*, 5847.

(16) Gordon, M. S., unpublished results.

(17) (a) Binkley, J. S.; Pople, J. A.; Hehre, W. J. *J. Am. Chem. Soc.* **1980**, *102*, 939. (b) Gordon, M. S.; Binkley, J. S.; Pople, J. A.; Pietro, W. J.; Hehre, W. J. *J. Am. Chem. Soc.* **1982**, *104*, 2797.

(18) Binkley, J. S.; Frisch, M. J.; DeFrees, D. J.; Krishnan, R.; Whiteside, R. A.; Schlegel, H. B.; Fluder, E. M.; Pople, J. A. GAUSSIAN82, Carnegie-Mellon Umiversity, Pittsburgh, PA, 1983.

(19) Schlegel, H. B. *J. Comput. Chem.* **1982**, *3*, 214.

(20) Ruedenberg, K.; Schmidt, M. W.; Gilbert, M. M.; Elbert, S. T. *Chem. Phys.* **1982**, *71*, 41. (b) Ruedenberg, K.; Schmidt, M. W.; Gilbert, M. M. *Chem. Phys.* **1982**, *71*, 51. (c) Ruedenberg, K.; Schmidt, Gilbert, M. M.; Elbert, S. T. *Chem. Phys.* **1982**, *71*, 65.

(21) Dupuis, M.; Spangler, D.; Wendoloski, J. J. NRCC Software Catalogue Program QG01, 1980.

(22) Schmidt, M. W.; Gordon, M. S.; Dupuis, M. *J. Am. Chem. Soc.* **1985**, *107*, 2585 and references cited therein.

(23) Pople, J. A.; Seeger, R.; Krishnan, R. *Int. J. Quantum Chem.* **1979**, *S11*, 149.

(24) Krishnan, R.; Frisch, M. J.; Pople, J. A. *J. Chem. Phys.* **1980**, *72*, 4244.

(25) Dunning, T. H., Jr. *J. Chem. Phys.* **1970**, *53*, 2823.

(26) McLean, A. D.; Chandler, G. S. *J. Chem. Phys.* **1980**, *72*, 5639.

(27) Krishnan, R.; Binkley, J. S.; Seeger, R.; Pople, J. A. *J. Chem. Phys.* **1980**, *72*, 650.

(28) Schmidt, M. W., private communication.

(29) Frisch, M. J.; Pople, J. A.; Binkley, J. S. *J. Chem. Phys.* **1984**, *80*, 3265.

(30) Woodward, R. B.; Hoffmann, R. *The Conservation of Orbital Symmetry*; Verlag Chemie: Weinheim/Bergstr., Germany, 1970.

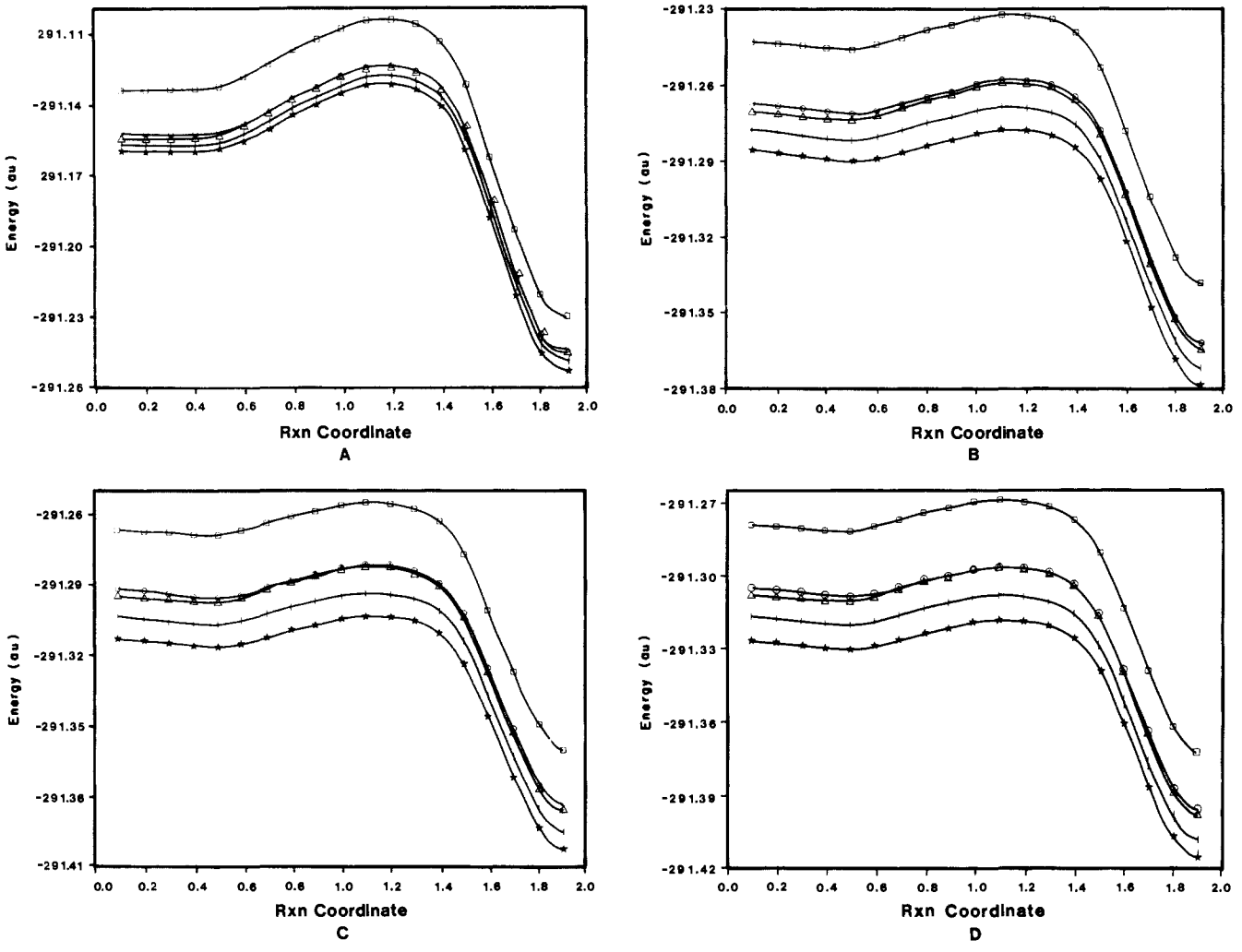

Figure 2. Energies (in Hartree) along the MCSCF IRC: (a) SCF; (b) MP2; (c) MP3; (d) MP4. In each set of curves, basis sets 6-31G**, A, B, C, and D are indicated by an open box, an open circle, a triangle, +, and −, respectively. Geometries chosen are available from the authors upon request.

Table I. Total Energies on SiH_4 Surface (Hartree)

		structure[a]			
method	basis set	R	W	S	P
SCF	6-31G**	−291.133 66		−291.104 04	−291.229 95
	A	−291.150 66	−291.152 53	−291.123 61	−291.248 98
	B	−291.152 85	−291.154 24	−291.123 78	−291.249 74
	C	−291.155 38	−291.156 90	−291.127 44	−291.252 42
	D	−291.158 14	−291.159 56	−291.130 81	−291.256 26
	E	−291.160 56	−291.159 98	−291.137 94	−291.259 44
MP2	6-31G**	−291.240 74	−291.246 13	−291.231 70	−291.399 09
	A	−291.262 52	−291.271 35	−291.258 01	−291.362 30
	B	−291.266 27	−291.273 63	−291.258 82	−291.364 46
	C	−291.273 11	−291.281 97	−291.268 53	−291.372 48
	D	−291.280 85	−291.290 16	−291.277 50	−291.379 86
	E	−291.301 97	−291.315 06	−291.305 14	−291.403 47
MP3	6-31G**	−291.264 50	−291.269 39	−291.255 24	−291.360 36
	A	−291.288 89	−291.295 76	−291.282 56	−291.384 38
	B	−291.290 91	−291.297 70	−291.282 88	−291.386 25
	C	−291.298 95	−291.307 27	−291.293 83	−291.395 90
	D	−291.308 12	−291.316 81	−291.303 72	−291.404 09
	E	−291.328 77	−291.341 02	−291.330 65	−291.427 85
MP4(STDQ)	6-31G**	−291.271 69	−291.276 27	−291.262 95	−291.366 06
	A	−291.295 10	−291.303 15	−291.290 86	−291.390 60
	B	−291.298 41	−291.304 92	−291.290 99	−291.392 31
	C	−291.306 68	−291.314 79	−291.302 23	−291.402 30
	D	−291.316 37	−291.324 82	−291.312 49	−291.410 90
	E	−291.337 11	−291.349 45	−291.339 49	−291.434 82

[a] R = reactants, W = well, S = saddle point, P = products.

Table II. Relative Energies on SiH_4 Surface (kcal/mol)

method	basis set	structure[a] R	W	S	P
SCF	6-31G**	0.0		18.6	-60.4
	A	0.0	-1.2	17.0	-61.7
	B	0.0	-0.9	18.2	-60.8
	C	0.0	-0.9	17.5	-60.9
	D	0.0	-0.9	17.1	-61.6
	E	0.0		14.2	-62.0
MP2	6-31G**	0.0	-3.4	5.7	-61.7
	A	0.0	-5.5	2.8	-62.6
	B	0.0	-4.6	4.7	-61.6
	C	0.0	-5.6	2.9	-62.3
	D	0.0	-5.8	2.1	-62.1
	E	0.0	-8.2	2.0	-63.7
MP3	6-31G**	0.0	-3.1	5.8	-60.1
	A	0.0	-4.3	4.0	-59.9
	B	0.0	-4.3	5.0	-59.8
	C	0.0	-5.2	3.2	-60.8
	D	0.0	-5.4	2.8	-60.2
	E	0.0	-7.7	-1.2	-62.2
MP4	6-31G**	0.0	-2.9	5.5	-59.2
	A	0.0	-5.0	2.7	-59.9
	B	0.0	-4.1	4.6	-58.9
	C	0.0	-5.1	2.8	-60.0
	D	0.0	-5.3	2.4	-59.3
	E	0.0	-7.7	-1.5	-61.3

[a] R = reactants, W = well, S = saddle point, P = products.

position of the transition state shifts slightly as a function of computational level, the energies given for point S correspond in each case to the highest point on the IRC. Similar comments apply to point W.

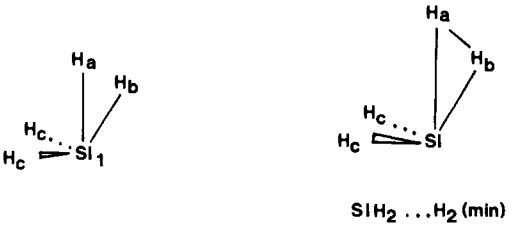

Figure 3. Schematics for the transition state and local minimum.

At the SCF level, the five basis sets (excluding basis E) predict a barrier between 17 and 19 kcal/mol, clearly too high as one would expect. As noted above, the four larger basis sets predict a very shallow long-range minimum of about 1 kcal/mol. Introduction of perturbation theory has a dramatic effect on both of these quantities: the size of the barrier is lowered to a range of 2–6 kcal/mol, and the depth of the long-range potential minimum increases to 3–5 kcal/mol, relative to the separated fragments. Generally, the trend appears to be a reduction of the barrier and a deepening of the well as the basis set is improved for a given level of perturbation theory. Because of this, MP2/6-311G(2d,2p) was used to reoptimize the geometries of the four key points. At this level of theory, points R, W, and P are verified as minima on the surface and point *S* as a transition state by virtue of the appropriate number of negative eigenvalues for the corresponding Hessian matrices (zero for minima, 1 for transition states). The structures of these four points are given in Table III and Figure 3. Included in Tables I and II are the energies at these points calculated with basis set E. The latter

Table III. MP2/MC-311G(2d,2p) Equilibrium Geometries, Total Energies (Hartree) and Harmonic Vibrational Frequencies (cm^{-1})

species	symmetry constraint	electronic state	geometrical[a] parameter	MP2/6-311G(2d,2p) total energy	harmonic symmetry of mode	freq
H_2	$D_{\infty h}$	$^1\Sigma_g$	r_{HH} 0.7365	-1.162800	Σ	4531
SiH_2	C_{2v}	$^1A_1$	r_{SiH} 1.5117	-290.251120	A_1	1047
			∠HSiH 92.07			2125
					B_2	2122
SiH_2	C_{2v}	$^3B_1$	r_{SiH} 1.4726	-290.226168	A_1	931
			∠HSiH 118.13			2265
					B_2	2330
SiH_3	C_{3v}	$^2A_1$	r_{SiH} 1.4747			
			∠HSiH 111.12	-290.865118	A_1	812
						2283
					E	979
						2313
SiH_4	T_d	$^1A_1$	r_{SiH} 1.4747	-291.512687	A_1	2309
					T2	966
						2311
					E	1019
$SiH_2\cdots H_2$ (TS)	C_s	$^1A'$	r_{SiH_a} 1.6364	-291.413891	A′	731
			r_{SiHb} 1.5149			996
			r_{SiH_c} 1.4765			1205i
			∠H_aSiH_b 42.00			1716
			∠H_aSiH_c 110.33			2288
			∠$H_aSi(H_c)$ 78.18			2199
			H_a–H_b 1.135		A″	774
						1062
						2307
$SiH_2\cdots H_2$ (well)	C_s	$^1A'$	r_{SiH_a} 1.8582	-291.424915	A′	609
			r_{SiH_b} 1.7866			788
			r_{SiH_c} 1.5052			1026
			∠H_aSiH_b 25.02			1368
			∠H_aSiH_c 94.92			2151
			∠$H_aSi(H_c)$ 65.63			3597
			H_a–H_b = 0.792		A″	477
						869
						2150

[a] Bond lengths in Å, angles in deg.

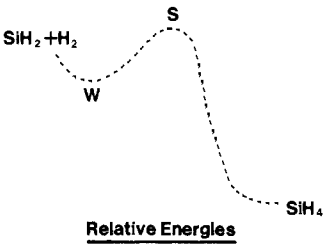

Relative Energies	Electronic	Total
SiH_2+H_2	0.0	0.0
W	-7.7	-3.1
S	-1.5	1.7
SiH_4	-61.3	-55.2

Figure 4. Summary of the energetics at the highest level of theory: MP4(SDTQ)/MC-311++G(3df,3pd)//MP2/MC-311G(2d,2p). Energies are in kcal/mol. Total energy refers to the sum of the electronic energy and zero-point correction.

continue the trend noted earlier, with the depth of the long-range well now being nearly 8 kcal/mol at the highest level of theory. At this same level, the saddle point is found to be 1.5 kcal/mol *below* the separated fragments and 6.2 kcal/mol above the long-range minimum. Clearly, point S represents a transition state separating points W and P.

The overall exothermicity of the reaction appears to be rather insensitive to both the basis set and the level of theory. Most of the entries in the last column of Table II lie between 60 and 62 kcal/mol. A direct comparison of all calculated energy quantities requires the incorporation of zero-point vibrational energies to be discussed below.

It is interesting to compare the structures of points R, W, and S given in Table III and Figure 3. The orientation of the two separating (or reacting) fragments is very similar in the well and at the saddle point, the major difference between the two, in fact, being the distance (L) between the fragments. If we take L to be the distance between Si and the midpoint of H_a–H_b, one finds L_e= 1.471 Å at the saddle point and 1.779 Å in the well. For comparison, L = 0.85 Å in silane. The H_a–H_b distance in the well is 0.792 Å. This is already stretched more than 0.05 Å, relative to H_2. This is a substantial amount and indicates the existence of strong electronic interactions between the two fragments, even at this large separation.

Also included in Table III are the vibrational frequencies of the various species involved in reaction 1. These may be used to calculate the zero-point vibrational corrections to the energy differences given in Table II for MP4(SDTQ)/E. The key results are summarized in Figure 4. Incorporation of the zero-point corrections reduces the depth of the well and raises the saddle point back above the separated fragments, yielding a calculated activation energy of 1.7 kcal/mol. Nonetheless, the long-range well is still found to lie nearly 5 kcal/mol below the transition state The overall endothermicity of the molecular dissociation is predicted to be 55.2 kcal/mol. The difference between this latter result and those of O'Neal and Ring is consistent with the difference in experimental and theoretical estimates of the heat of formation of silylene. It is noteworthy, however, that the calculated energetics presented here are consistent with both the recent experimental results of Jasinski and Estes[6] and the semiempirical model of Viswanathan and co-workers.[7]

In order to compare the molecular elimination of hydrogen with the homolytic fragmentation of silane to yield silyl radical, the geometry and energy of the latter are also included in Table III. The electronic energy required for this homolytic cleavage is calculated to be 95.4 kcal/mol. Incorporation of zero-point energy differences reduces this value to 89.2 kcal/mol. The latter is in excellent agreement with Walsh's estimate of 90 kcal/mol for the SiH bond energy[31] and supports the point made earlier that cleavage of this bond is much less likely at low energies than the molecular elimination.

IV. Conclusions

The essential features of the potential energy surface for the thermal decomposition of silane have been presented at a high level of theory. It is predicted that the transition state for the molecular elimination lies 56.9 kcal/mol above silane, a value which is within the experimental error bars of Jasinski and Estes.[6] With regard to the reverse reaction, the transition state is less than 2 kcal/mol above the separated fragments, silylene and molecular hydrogen, but 4.8 kcal/mol above a long-range potential well. In the latter the silylene–H_2 separation is 1.78 Å, and the bond in H_2 has stretched by more than 0.05 Å. This indicates a significant electronic interaction between the fragments even at the large fragment separation. The depth of the well is only 1 kcal/mol or less at the SCF level of theory, but it increases substantially when correlation is introduced into the wave function. This suggests that the well arises primarily as a result of van der Waals type interactions.

The energy difference between the separated fragments and the transition state is much less than the earlier experimental estimates[3,4] but in agreement with the more recent work of Jasinski.[6b] The disagreement with the earlier experiments may be traced to the similar disparity between the experimental and theoretical estimates of the heat of formation of silylene. The calculated SiH bond energy is in excellent agreement with the experimental value found for this quantity by Walsh. Since it is 22 kcal/mol larger than the activation energy for the molecular elimination, the homolytic cleavage of silane to form silyl radical is not expected to be an important process in the low-energy pyrolysis of silane.

Acknowledgment. This work was supported in part by grants to M.S.G. by the donors of the Petroleum Research Fund, administered by the American Chemical Society, and by the National Science Foundation (CHE83-09948). The computer time made available by the computer centers at Sandia National Laboratory and North Dakota State University is gratefully acknowledged. The authors are also indebted to Dr. Joe Jasinski for making his recent experimental findings available prior to publication.

Registry No. SiH_4, 7803-62-5.

(31) Walsh, R. *Acc. Chem. Res.* **1981**, *14*, 246.